Biosensors and Bioelectronics 64 (2015) 13–18

Contents lists available at ScienceDirect

Biosensors and Bioelectronics

journal homepage: www.elsevier.com/locate/bios

Label-free photoelectrochemical immunosensor for sensitive detection of Ochratoxin A

Jiaojiao Yang [a], Picheng Gao [a], Yixin Liu [a], Rongxia Li [b], Hongmin Ma [a], Bin Du [a,b,*], Qin Wei [a]

[a] Key Laboratory of Chemical Sensing & Analysis in Universities of Shandong, School of Chemistry and Chemical Engineering, University of Jinan, Jinan 250022, PR China

[b] School of Resources and Environmental Sciences, University of Jinan, Jinan 250022, PR China

ARTICLE INFO

Article history:
Received 1 July 2014
Received in revised form
13 August 2014
Accepted 14 August 2014
Available online 19 August 2014

Keywords:
TiO_2
CdSe
Label-free
Ochratoxin A
Photoelectrochemical sensor

ABSTRACT

A general label-free photoelectrochemical (PEC) platform was manufactured by assembly of CdSe nanoparticles (NPs) sensitized anatase TiO_2-functionalized electrode *via* layer-by-layer (LBL) strategy. CdSe NPs were assembled on anatase TiO_2-functionalized electrode through dentate binding of TiO_2 NPs to –COOH groups. Ascorbic acid (AA) was used as an efficient electron donor for scavenging photogenerated holes under visible-light irradiation. The photocurrent response of the CdSe NPs modified electrode was significantly enhanced as a result of the band alignment of CdSe and TiO_2 in electrolyte. Ochratoxin A (OTA), as model analyte, was employed to investigate the performance of the PEC platform. Antibodies of OTA were immobilized on CdSe sensitized electrode by using the classic 1-ethyl-3-(3-dimethylaminopropyl) carbodiimide hydrochloride coupling reactions between –COOH groups on the surfaces of CdSe NPs and $–NH_2$ groups of the antibody. Under the optimized conditions, the photocurrent was proportional to OTA concentration range from 10 pg/mL to 50 ng/mL with detection limit of 2.0 pg/mL. The employed PEC platform established a simple, fast and inexpensive strategy for fabrication of label-free biosensor, which might be widely applied in bioanalysis and biosensing in the future.

1. Introduction

Photoelectrochemical (PEC) assay based on a photoelectric chemical phenomenon has been widely applied in chemical analysis by reason of its high sensitivity, low-cost and low background current (Brown et al., 1992; Li et al., 2012; Zheng et al., 2011). In principle, PEC can be viewed as the inverse process of electroluminescence (ECL) (Cui et al., 2003; Richter, 2004), which exhibits charge-transfer upon photoexcitation and achieves the detection purpose *via* the intensity of the photocurrent. PEC sensors have the advantages of both optical and electrochemical (Ikeda et al., 2009). Many groups have devoted much efforts in developing a novel PEC sensor for detection of chemicals and biomolecules (Yue et al., 2013).

Semiconductor is the key material in fabricating PEC sensor. As a kind of semiconductor material, TiO_2 is generally utilized in the photocatalysis and photoelectrochemistry due to its availability, nontoxicity, photostability and high electronic mobility (Fujishima and Honda, 1972). There are three main kinds of crystalline structure of TiO_2: anatase, brookite, and rutile. The difference of these three crystal structures induces tremendous diversity on the physical properties, so it leads to their specially applied field (Wang et al., 2008). Anatase phase with a high photocatalytic activity is usually used in photocatalysis (Berger et al., 2005). Yet, TiO_2 is a kind of wide band-gap semiconductor material and only has a PEC activity under ultra-violet irradiation (Wold, 1993), these features have taken a toll on its application in photoelectrochemistry. Therefore, either narrowing the band gap of TiO_2 to allow the absorption in the visible region or decreasing the electron/hole recombination is being considered. CdSe nanoparticles (NPs) are an ideal sensitizing material with a narrow-band gap and broad excitation spectrum (Cordes et al., 2006; Díaz et al., 2013); combining that with TiO_2 could greatly improve the photocurrent intensity and photostability of TiO_2 due to the enhanced charge separation efficiency (Nasr et al., 1998; Sant and Kamat, 2002).

Herein, a label-free PEC platform was developed by assembly of CdSe NPs sensitized anatase TiO_2-functionalized electrode *via* layer-by-layer (LBL) strategy. Indium tin oxide (ITO) electrode was functionalized by dropping TiO_2 NPs and calcination induced formation of normalized anatase crystalline structure. Ochratoxin A (OTA) was used as a model analyte in order to investigate the

* Corresponding author at: School of Resources and Environmental Sciences, University of Jinan, Jinan 250022, PR China.
Tel./fax: +86 531 8276 7370.
E-mail address: dubin61@gmail.com (B. Du).

http://dx.doi.org/10.1016/j.bios.2014.08.025
0956-5663/

performance of the PEC sensor. OTA is a secondary metabolite produced by the genera aspergillus and penicillium (Van der Merwe et al., 1965); it is well known as a fungaltoxin existing in various kinds of foods, fodders, and other agricultural and sideline products (Fernández-Cruz et al., 2010). OTA is the most toxic compound in the ochratoxins group, which has a high chemical stability and thermal stability. With the development of toxicology, studies have shown that OTA is a nephrotoxin, hepatotoxin, carcinogen and teratogen (Heurich et al., 2011; Petzinger and Weidenbach, 2002). Many methods have been applied to detect OTA, such as high performance liquid chromatography (HPLC) (Soleas et al., 2001), high performance liquid chromatography with fluorescence detection (HPLC-FD) (Rhouati et al., 2011), and enzyme linked immunosorbent assay (ELISA) (Heurich et al., 2011). Nevertheless, these methods are expensive, time consuming and demanded the sample to be labeled (Van der Gaag et al., 2003). To the best of our knowledge, this is the first time to determine OTA through label-free PEC method. CdSe NPs with narrow band gap was modified on TiO_2-functionalized ITO electrode *via* dentate binding of TiO_2 NPs to –COOH groups and significantly improve photo-to-electric efficiency of the electrode. Besides, ascorbic acid (AA) acted as an electron donor for scavenging photogenerated holes and could obviously enhance PEC response. The proposed label-free PEC platform opens a new era for sensitive detection of chemicals and biomolecules.

2. Experimental section

2.1. Materials

OTA and OTA antibody were purchased from Wanger Biotechnology Co., Ltd. (Beijing, China). AA, cadmium chloride ($CdCl_2 \cdot 2.5H_2O$) was acquired from Sinopharm Chemical Reagent Co., Ltd. (Shanghai, China). Thioglycolic acid (TGA) was obtained from Tianjin Kermel Chemical Reagent Co., Ltd. (Tianjin, China), bovine serum albumin (BSA), N-hydroxysuccinimide (NHS) and 1-ethyl-3-(3-dimethylaminopropyl) carbodiimide hydrochloride (EDC) were obtained from Aladdin Reagent Database Inc. (Shanghai, China). All other chemicals were of analytical reagent grade and were used without further purification. Phosphate buffered saline (PBS) were prepared using 0.1 mol/L Na_2HPO_4 and 0.1 mol/L KH_2PO_4 stock solution. Ultrapure water (18.25 MΩ cm, 24 °C) was used throughout the experiment.

2.2. Apparatus

All PEC measurements were carried out with a home-built PEC system. A common low-cost 30 W LED lamp was used as an irradiation source. Photocurrent was measured on a CHI 760D electrochemical workstation (Chenhua Instrument Shanghai Co., Ltd., China) using a three-electrode system which consisted of a platinum wire as a counter-electrode, a saturated calomel electrode as reference electrode and a modified TiO_2-functionalized ITO electrode as the working electrode. Electrochemical impedance spectroscopy (EIS) was obtained from IM6&Zennium electrochemical workstation (Zahner, Germany). Transmission electron microscope (TEM) image was obtained from an H-800 microscope (Hitachi, Japan). Scanning electron microscope (SEM) image was obtained using a field emission SEM (ZEISS, Germany). X-ray diffraction (XRD) patterns were performed with D8 advance X-ray diffractometer (Bruker AXS, Germany). Fourier transform infrared (FTIR) spectrum was obtained with a Perkin-Elmer 580B spectrophotometer (Perkin-Elmer, United States).

2.3. Preparation of TiO_2-functionalized ITO electrode

Before biosensor fabrication, the TiO_2 NPs were prepared according to the literature (Huang et al., 2013). 0.02 mol of tetrabutyl orthotitanate was dissolved into 30 mL of ethanol, following by adding 10 mL distilled water under magnetic stirring, After stirring for another 120 min, the suspension was transferred to the reaction kettle and maintained on the blast oven at 200 °C for 10 h. The obtained white precipitates were washed completely with distilled water and ethanol for five times and then dried in vacuum at 80 °C for 12 h to get the TiO_2 NPs.

ITO substrates were cut into $3.0 \times 0.8\ cm^2$ pieces and then cleaned ultrasonically in ultrapure water, acetone, ethanol and ultrapure water for 30 min, consecutively. After being dried with a stream of N_2, 6 μL TiO_2 solution which was sonicated in water for 60 min was dropped onto a piece of ITO slice. The film was dried under an infrared lamp, followed by calcination at 450 °C for 30 min in a muffle oven, and then placed for a while to cool down to room temperature.

2.4. Preparation of TGA-stabilized CdSe NPs

The water-soluble CdSe NPs were synthesized according to the reported method (Zhang et al., 2011). Briefly, dissolving 10 mmol Se powder and 12 mmol Na_2SO_3 in 50 mL ultrapure water under magnetic stirring at 90 °C for 3 h will get the Na_2SeSO_3 solution. Then, 0.84 mL TGA diluted with 60 mL distilled water was added into 40 mL of 0.125 mol L^{-1} $CdCl_2 \cdot 2.5H_2O$ solution under magnetic stirring. Thereafter, the pH value of the solution was adjusted to 10 with 1.0 mol L^{-1} NaOH. 12 mL of the obtained Na_2SeSO_3 solution was added into the above solution. The solution was heated to boiling and refluxed for 4 h.

2.5. Fabrication of PEC biosensor via LBL strategy

Fabrication process of the proposed label-free PEC immunosensor is shown as Scheme 1. Generally, 3 μL TGA-stabilized CdSe NPs solution was dropped and immobilized on the TiO_2-functionalized ITO electrode through dentate binding of TiO_2 NPs to –COOH groups. 3 μL EDC/NHS solution was dropped on CdSe/TiO_2 /ITO electrode to activate –COOH on the surfaces of the TGA-capped CdSe NPs. After washing the unbound EDC/NHS with deionized water, 3 μL OTA antibodies (anti-OTA) were introduced to the modified electrode surface and followed by rinsing with distilled water to remove the loosely bounded anti-OTA. Subsequently, 1% BSA was employed as the blocking buffer solution to

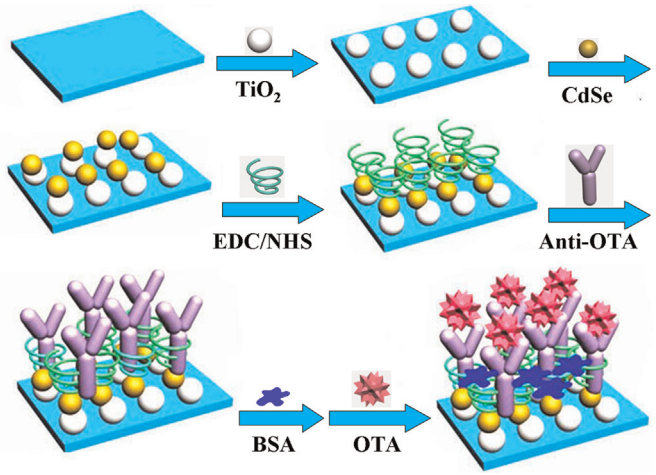

Scheme 1. Schematic illustration of the PEC immunosensor fabrication process.

block nonspecific binding sites. After being washed with care, the electrode was used as a PEC platform for detection of OTA and placed at 4 °C while unused.

3. Results and discussion

3.1. Morphological and spectroscopic characterization of TiO_2 and CdSe

ITO substrate electrode was functionalized by TiO_2 NPs and calcination to ensure rigid immobilization of TiO_2 NPs. SEM image (Fig. 1A) shows rough and close packing morphology of TiO_2 -functionalized electrode; TiO_2 NPs were evenly distributed on the surface of ITO, which is beneficial for the subsequent conjugation of TGA-capped CdSe NPs and available for the electron transfer from CdSe to TiO_2 (Zhao et al., 2011). TEM image (Fig. 1B) of TiO_2 NPs reveals that the average size of TiO_2 NPs is ~10 nm; small size induced large specific surface area allows sufficient loading of CdSe and improves photon absorption and harvesting efficiency. The high crystallinity and phase purity of the resultant TiO_2 NPs were confirmed by the XRD pattern (Fig. 1C, curve a). The distinct peaks match well with the pure anatase TiO_2 (JCPDS Card no. 21-1272) (Tang and Li, 2008). After annealed at 450 °C for 30 min (Fig. 1C, curve b), intenser peaks of the pattern imply higher degree crystalline structure of anatase TiO_2 (Yuan et al., 2014). The reason might be that annealing temperature (450 °C) is higher than hydrothermal reaction temperature (180 °C) and is beneficial for the formation of more standard anatase phase. Average size of CdSe NPs is ~2 nm (Fig. 1D). The small CdSe particles could be homogeneously dispersed on the TiO_2 film surface (Zhao et al., 2011). Fig. 1E shows the FT-IR spectrum of TGA-capped CdSe in the wavenumber range from 500 to 3750 cm^{-1}. The strong absorption peak at 1396 cm^{-1} is characteristic of the C=O stretching vibration of carboxylic group. A relatively weak peak at 1635 cm^{-1} is the O–H bending vibration. The broad band at 3160 cm^{-1} may be ascribed to the O–H stretching vibration of carboxyl (Dong et al., 2013). The results confirm the preservation of carboxyl group in CdSe and prove the possibility of CdSe NPs immobilized on TiO_2-functionalized ITO electrode through dentate binding of TiO_2 NPs to –COOH groups.

3.2. Characterization of the fabricated PEC immunosensor

To illustrate the fabrication process of the PEC immunosensor, the EIS was studied with various electrodes in 2.5 mmol/L $K_3Fe(CN)_6+K_4Fe(CN)_6$ solution. The electrochemical impedance Nyquist plots of diverse modified electrodes are shown in Fig. 2A. Compared with bare ITO electrode (curve a), the semicircle diameter significantly increased after the electrode was modified with TiO_2 (curve b), which indicates that TiO_2 NPs were successfully anchored on the surface of ITO electrode and inhibited electron transfer of the system. Obvious increased electron-transfer resistance (curve c) suggested that TGA-capped CdSe NPs were conjugated on TiO_2-functionalized electrode *via* dentate binding of TiO_2 NPs to –COOH groups (Tu et al., 2009). Subsequently, the electrode was combined with EDC/NHS that was used for linking the –COOH groups of CdSe NPs and $-NH_2$ groups of anti-OTA; the diameter of the semicircle is further increased due to the insulation of EDC/NHS (curve d). When the electrode was conjugated with anti-OTA (curve e) and blocked with BSA (curve f), the resistance of the electrode increased greatly, followed by the semicircle increased. The results indicate the successfully immobilization of antibody and BSA. The further multiplied electron-transfer resistance (curve g) confirmed that the OTA was triumphantly incubated with anti-OTA; the results suggest that the

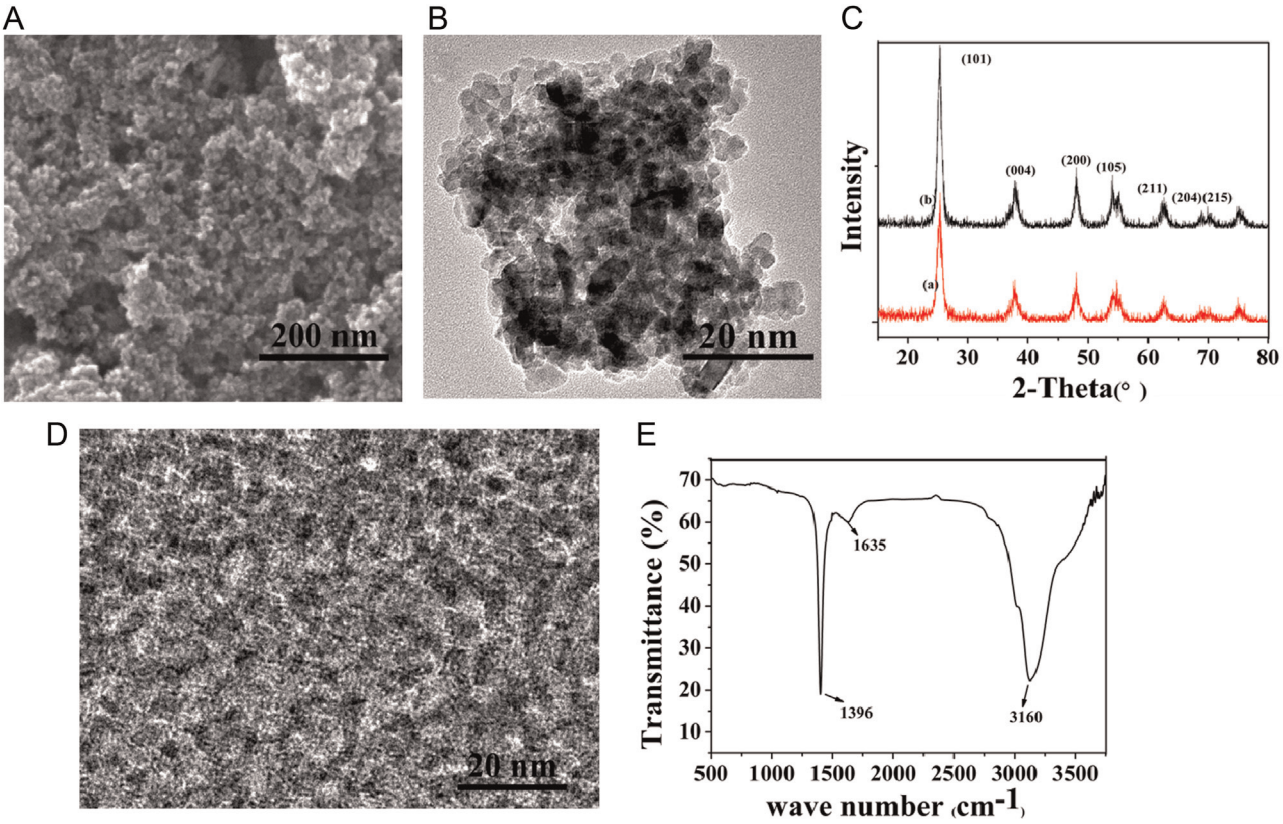

Fig. 1. (A) SEM image and (B) TEM image of TiO_2 NPs, (C) XRD patterns of TiO_2 NPs before (curve a) and after (curve b) calcination. (D) TEM image and (E) FT-IR spectrum of CdSe NPs.

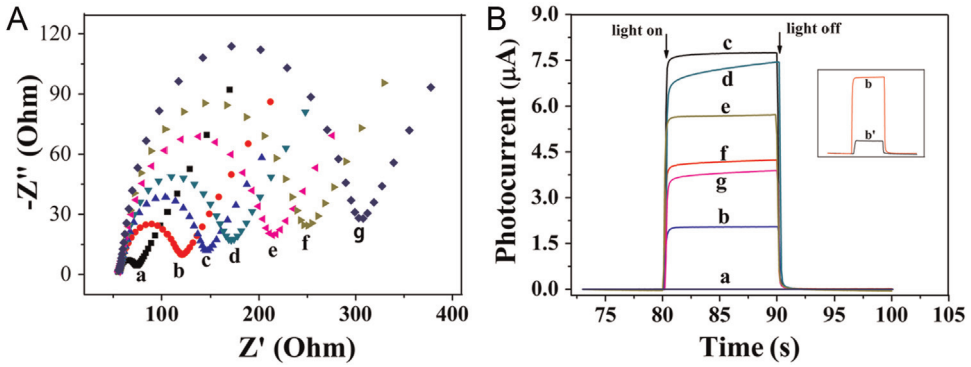

Fig. 2. (A) Nyquist diagrams and (B) photocurrent response of different electrodes. (a) ITO, (b) TiO_2/ITO, (c) CdSe/TiO_2/ITO, (d) (EDC/NHS)/CdSe/TiO_2/ITO, (e) anti-OTA/(EDC/NHS)/CdSe/TiO_2/ITO, (f) BSA/anti-OTA/(EDC/NHS)/CdSe/TiO_2/ITO, and (g) OTA/BSA/anti-OTA/(EDC/NHS)/CdSe/TiO_2/ITO. The applied potential was 0 V. Inset in (B) shows the photocurrent response of TiO_2/ITO electrode before (b′) and after (b) calcinations.

immobilized OTA on the electrode could retain their native bioactivity and the fabricated PEC platform could be applied for the determination of OTA.

As mentioned above, CdSe sensitized anatase TiO_2-functionalized ITO electrode was used as the PEC platform for the fabrication of OTA immunosensor. High photo-to-electron conversion of semiconductor is essential in achieving a high sensitivity of PEC sensor. First of all, AA was used as a photo-generated hole scavenger to suppress photo-excited electron–hole recombination under visible-light irradiation. In order to further confirm the successful immobilization of corresponding material and illustrate PEC performance of the immunosensor, photocurrent response under visible light illumination of each step modified electrode was investigated and is shown in Fig. 2B. No photo to electric conversion occurred on bare ITO electrode (curve a) and photocurrent was collected once the TiO_2-functionalized electrode was exposed under visible light (curve b). Interestingly and particularly worth mentioned, after calcination, photocurrent response of the TiO_2-functionalized ITO electrode significantly improved (inset in Fig. 2B), which might be due to the formation of more standard anatase phase. CdSe NPs are a narrow band gap semiconductor (1.7 eV) (Wang et al., 2010); it showed higher electron–hole separation efficiency than TiO_2 under visible light. Assembled CdSe NPs on TiO_2-funtionalized ITO electrode result in nearly 5 times enhancement of photocurrent response. As the Fermi levels of CdSe and TiO_2 are aligned, the electron created in CdSe can be injected to conduction band of TiO_2, which can decrease the recombination efficiency of photo-generated electron and hole of TiO_2 and improve photocurrent response of TiO_2-functionalized electrode (Scheme 2). However, the photocurrent decreased slightly for EDC/NHS immobilization (curve d), which was due to insulation property of EDC/NHS. Subsequently, the photocurrent intensity tapered after the assembling of anti-OTA (curve e) and BSA (curve f). The decrease in the photocurrent could be explained by the fact that the immobilized biomacromolecule partly hampered the electron-transfer from AA to CdSe and resulted in the recombination of photo-generated holes and electrons. By monitoring the photocurrent decrease after the modification of OTA (curve g), a label-free PEC immunosensor was achieved.

3.3. Optimization of experimental conditions

In order to obtain the best performance for PEC detection of OTA, experiment conditions were optimized. Influences of the TiO_2 concentration on the PEC response were investigated by preparing different concentrations of TiO_2 suspensions (Fig. 3A). With the increase of the TiO_2 concentration from 0.5 to 2.0 mg/mL, the photocurrent intensity was increased gradually. However, the

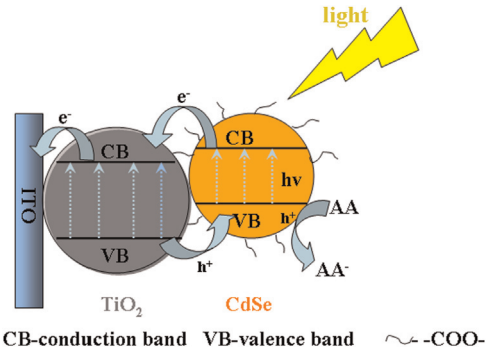

Scheme 2. Schematic illustration of CdSe sensitized TiO_2 PEC mechanism.

photocurrent intensity decreased when the concentration of TiO_2 further increased. Increasing concentration of TiO_2 suspension could increase the thickness of the TiO_2 film (Kuang et al., 2006), which would generate more photoactive materials and light absorption (Li et al., 2012). Nevertheless, the thicker TiO_2 film could also result in the increase of diffusion resistance for electron motion, followed by the decrease of photocurrent (Wang et al., 2009). Therefore, 2.0 mg/mL TiO_2 suspension was chosen as the optimal concentration for the following experiments.

AA was used as an electron donor to suppress the electron–hole recombination of CdSe sensitized TiO_2-functonalized electrode and therefore obtained enhanced and stable photocurrent intensity. The effect of the AA concentrations on the photocurrent responses was studied in the range from 0.00 to 0.20 mol/L (Fig. 3B). With the increase of concentration up to 0.1 mol/L, the photocurrent increased. The lower responses at the concentration higher than 0.1 mol/L might be primarily due to the saturation of electron donor. Thus, 0.1 mol/L AA was employed as the optimum concentration of electron donor for the subsequent experiments.

In order to obtain an optimal PEC signal, the pH value of buffer solution was also investigated. As shown in Fig. 3C, the immunosensor achieved a maximum value at pH 7.0; overly acidic or basic detection surroundings might damage the activity of the immobilized protein (Yuan et al., 2004). Hence, PBS with a pH of 7.0 was selected as the optimal condition throughout this immunoassay.

3.4. Immunosensor performance

The developed PEC immunosensor was applied to detect different concentrations of OTA under the optimized conditions (Fig. 3D). The photocurrent intensity was proportional to the logarithm of OTA concentration in the range from 0.01 ng/mL to 50.00 ng/mL, and the equation of the calibration curve is

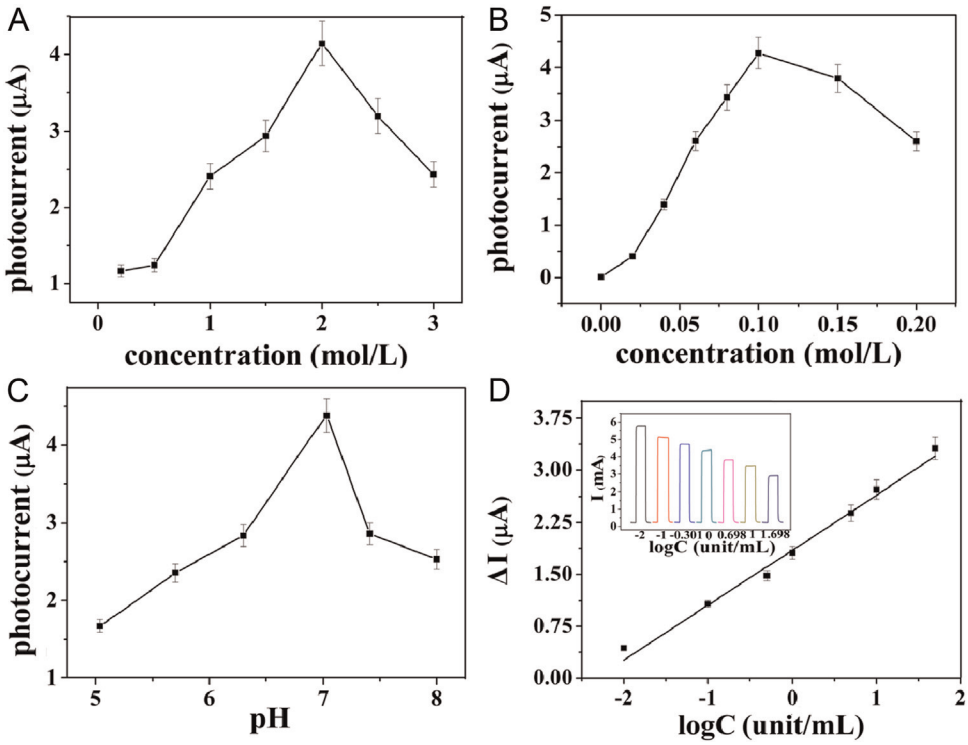

Fig. 3. Effects of (A) concentrations of TiO_2 suspension, (B) AA concentrations and (C) pH of the substrate solution on the photocurrent response of the OTA immunosensor. (D) Photocurrent responses of the PEC biosensor after treatment with various concentrations of OTA ($\Delta I = I_0 - I$, I_0 is the photocurrent response of blank experiment and I is the current of solution containing antigen).

$\Delta I = 1.8793 + 0.7871$ lg[c], $R = 0.9873$. The limit of detection was estimated to be 2.0 pg/mL (3 s/k, s is standard deviations of the blank ($n = 10$); k is the slope of the calibration curve line), which is lower than that in some previous reports (Table S1). The low detection limit may be attributed to the fact that a large amount of antibody has been conjugated on the CdSe nanoparticles because of the large surface area of CdSe and TiO_2, which could increase the probability of antibody–antigen interactions, and the low background signal of PEC detection also leads to the higher sensitivity.

3.5. Stability, reproducibility and selectivity

The stability of the photocurrent responses of the fabricated biosensor was assessed and displayed in Fig. S1A. No noticeable change of photocurrent response was recorded with the excitation light on and off, which was repeated 19 times with the interval of 10 s, indicating the excellent stability of the proposed immunosensor.

To examine the reproducibility of the biosensor, five electrodes were prepared for the detection of 1.0 ng/mL OTA. All the tests were performed under the same conditions with the relative standard deviation (RSD) of 1.2%. The results suggested that the precision and reproducibility of immunosensor were fairly satisfactory.

The selective determination of the immunosensor was carried out under the optimal conditions using estrodiol, aflatoxin and vomitoxin. 1.0 ng/mL of OTA solution containing 100 ng/mL of interfering substances was measured; no obvious change in current was obtained in comparison with the result observed in the presence of OTA only, and the RSD of the measurement was 1.1% (Fig. S1B). The results indicated that the biosensor has a good selectivity.

3.6. Real sample analysis

In order to study the feasibility of the biosensor for a real sample, the proposed immunosensor was used to detect the recoveries of different concentrations (5.00, 10.0, and 20.0 ng/mL) of OTA in milk by standard addition methods. As shown in Table 1, the recovery was in the range of 98.6–107.9% and RSD was in the range of 1.7–2.7%, Hence, the fabricated immunosensor was satisfied.

4. Conclusions

A general label-free photoelectrochemical platform based on CdSe sensitized anatase TiO_2-functionalized electrode was proposed and applied in sensitive detection of OTA under visible-light irradiation. CdSe NPs were bonded on TiO_2-functionalized

Table 1
The result of OTA determination in milk by the proposed immunosensor.

Content of OTA in the milk (ng/mL)	The addition content (ng/mL)	The detection content (ng/mL)	Average value (ng/mL)	RSD (%)	Recovery (%)
27.28	5.00	33.40 31.25 32.41 33.22 33.10	32.68	2.7	107.9
	10.0	37.29 36.44 36.20 37.36 38.40	37.14	2.3	98.6
	20.0	47.37 46.23 48.11 46.96 48.20	47.37	1.7	100.5

electrode *via* dentate binding of TiO_2 NPs to –COOH groups rather than a simple physical adsorption. The results demonstrated that CdSe NPs possess a strong inhibition to the recombination of the photogenerated carriers and markedly improve the photocurrent response of TiO_2-functionalized electrode. OTA was used as model analyte and exhibits wide linear range (10.0 pg/mL–50.0 ng/mL), low detection limit (2.0 pg/mL), satisfying selectivity, reproducibility and acceptable stability. Also, this method has the advantages of simple equipment and convenient operation, which provides a novel strategy for fabrication of PEC sensor for detection of chemicals and biomolecules.

Acknowledgments

This study was supported by the National Natural Science Foundation of China (Nos. 21175057, 21203074, 21375047, and 21377046), the Science and Technology Plan Project of Jinan (No. 201307010), and QW thanks the Special Foundation for Taishan Scholar Professorship of Shandong Province and UJN (No. ts20130937).

Appendix A. Supplementary information

Supplementary data associated with this article can be found in the online version at http://dx.doi.org/10.1016/j.bios.2014.08.025.

References

Berger, T., Sterrer, M., Diwald, O., Knözinger, E., Panayotov, D., Thompson, T., Yates, J., 2005. J. Phys. Chem. B 109, 6061–6068.
Brown, G.N., Birks, J.W., Koval, C.A., 1992. Anal. Chem. 64, 427–434.
Cordes, D.B., Gamsey, S., Singaram, B., 2006. Angew. Chem. Int. Ed. 45, 3829–3832.
Cui, H., Zou, G.-Z., Lin, X.-Q., 2003. Anal. Chem. 75, 324–331.
Díaz, S. n. A., Giordano, L., Azcárate, J.C., Jovin, T.M., Jares-Erijman, E.A., 2013. J. Am. Chem. Soc. 135, 3208–3217.
Dong, Y., Chen, C., Lin, J., Zhou, N., Chi, Y., Chen, G., 2013. Carbon 56, 12–17.
Fernández-Cruz, M.L., Mansilla, M.L., Tadeo, J.L., 2010. J. Adv. Res. 1, 113–122.
Fujishima, A., Honda, K., 1972. Nature 238, 37–38.
Heurich, M., Kadir, M.K.A., Tothill, I.E., 2011. Sens. Actuators B: Chem. 156, 162–168.
Huang, Q., Tian, S., Zeng, D., Wang, X., Song, W., Li, Y., Xiao, W., Xie, C., 2013. ACS Catal. 3, 1477–1485.
Ikeda, A., Nakasu, M., Ogasawara, S., Nakanishi, H., Nakamura, M., Kikuchi, J.-i., 2009. Org. Lett. 11, 1163–1166.
Kuang, D., Ito, S., Wenger, B., Klein, C., Moser, J.-E., Humphry-Baker, R., Zakeeruddin, S.M., Grätzel, M., 2006. J. Am. Chem. Soc. 128, 4146–4154.
Li, Y.J., Ma, M.J., Zhu, J.J., 2012. Anal. Chem. 84, 10492–10499.
Nasr, C., Kamat, P.V., Hotchandani, S., 1998. J. Phys. Chem. B 102, 10047–10056.
Petzinger, E., Weidenbach, A., 2002. Livest. Prod. Sci. 76, 245–250.
Rhouati, A., Paniel, N., Meraihi, Z., Marty, J.-L., 2011. Food Control 22, 1790–1796.
Richter, M.M., 2004. Chem. Rev. 104, 3003–3036.
Sant, P.A., Kamat, P.V., 2002. Phys. Chem. Chem. Phys. 4, 198–203.
Soleas, G.J., Yan, J., Goldberg, D.M., 2001. J. Agric. Food Chem. 49, 2733–2740.
Tang, X., Li, D., 2008. J. Phys. Chem. C 112, 5405–5409.
Tu, W., Lei, J., Ding, L., Ju, H., 2009. Chem. Commun. 28, 4227–4229.
Van der Gaag, B., Spath, S., Dietrich, H., Stigter, E., Boonzaaijer, G., van Osenbruggen, T., Koopal, K., 2003. Food Control 14, 251–254.
Van der Merwe, K., Steyn, P., Fourie, L., Scott, D.B., Theron, J., 1965. Nature 205, 1112–1113.
Wang, G.-L., Xu, J.-J., Chen, H.-Y., Fu, S.-Z., 2009. Biosens. Bioelectron. 25, 791–796.
Wang, G., Yang, X., Qian, F., Zhang, J.Z., Li, Y., 2010. Nano Lett. 10, 1088–1092.
Wang, X., Mitchell, D.R., Prince, K., Atanacio, A.J., Caruso, R.A., 2008. Chem. Mater. 20, 3917–3926.
Wold, A., 1993. Chem. Mater. 5, 280–283.
Yuan, L., Yu, Z., Li, C., Li, J., Shen, Y., Zhang, H., Wang, C., Xie, A., 2014. J. Electrochem. Soc. 161, H332–H336.
Yuan, R., Tang, D., Chai, Y., Zhong, X., Liu, Y., Dai, J., 2004. Langmuir 20, 7240–7245.
Yue, Z., Lisdat, F., Parak, W.J., Hickey, S.G., Tu, L., Sabir, N., Dorfs, D., Bigall, N.C., 2013. ACS Appl. Mater. Interfaces 5, 2800–2814.
Zhang, X., Li, S., Jin, X., Li, X., 2011. Biosens. Bioelectron. 26, 3674–3678.
Zhao, W.-W., Yu, P.-P., Xu, J.-J., Chen, H.-Y., 2011. Electrochem. Commun. 13, 495–497.
Zheng, M., Cui, Y., Li, X., Liu, S., Tang, Z., 2011. J. Electroanal. Chem. 656, 167–173.